Polymers for Advanced Technologies, Vol. 28, Issue 11, November 2017, pp. 1375-1381
DOI:10.1002/pat.4014

Synthesis, Characterization and Functionalization of Zirconium Tungstate (ZrW_2O_8) Nano-rods for Advanced Polymer Nanocomposites

Vijay Kumar Thakur[1*], Yuzhan Li[2], Hongchao Wu[3], and Michael R. Kessler[2*]

[1]Enhanced Composites & Structures Centre, School of Aerospace, Transport and Manufacturing, Cranfield University, Cranfield, Bedfordshire MK43 0AL, England (UK)

Email: Vijay.Kumar@cranfield.ac.uk; T: +44 (0) 1234 750111 x2344

[2]*School of Mechanical and Materials Engineering, Washington State University, Pullman, Washington 99164, United States*

Email: michaelr.kessler@wsu.edu; T: +1 (0) 509 335 8491

[3]*Department of Materials Science and Engineering, Iowa State University, Ames, Iowa 50011, United States*

ABSTRACT

Nano-materials based on zirconium tungstate (ZrW_2O_8) exhibit numerous outstanding properties that make them ideal candidates for the development of high-performance composites. Low coefficient of thermal expansion (CTE) for advanced materials is a promising direction in the field of insulating nanocomposites. However, the agglomeration of zirconium tungstate (ZrW_2O_8) based nano-materials in the polymer matrix is a limiting factor in their successful applications and studies on surface functionalization ZrW_2O_8 for advanced nanocomposites are very limited. In this work, ZrW_2O_8 nano-rods were synthesized using a hydrothermal method and subsequently functionalized in a solvent-free aqueous medium using dopamine. Both pristine and

functionalized nano-rods were thoroughly characterized using FTIR, Raman, TGA, XRD, SEM, and TEM techniques which confirmed the successful functionalization of the nanomaterials. Polymer nanocomposites were also prepared using epoxy resin as a model matrix. Polymer nanocomposites with functionalized ZrW_2O_8 nano-rods exhibited low CTE and enhanced tensile properties. The improved properties of the nanocomposites render them suitable for electronic applications.

Keywords: Mussel-inspired functionalization; negative CTE; thermosetting resins; polymer matrix nanocomposites; mechanical properties.

1. INTRODUCTION

Polymer-based materials are often used in combination with ceramic and metallic materials because of their excellent properties such as ease of processing and tailoring, low cost, flexibility, among others [1][2][3]. Polymer-based composite materials are currently used for a wide variety of applications, in particular in the aerospace, automotive, and energy industries owing to their durability, dimensional stability, high specific strength to weight ratio, and improved corrosion resistance [4][5][6]. Among other materials, epoxy-based composites are widely used in adhesive, construction, aerospace, and satellite applications [7][8][9]. Epoxy-based polymers exhibit excellent properties in terms of adhesion, chemical and heat resistance, as well as superior mechanical/insulating properties [10]. Different reinforcing materials are used to increase the properties of the epoxy resin in the composite [11][12]: E-glass increases the bearing strength of epoxy laminates [13]; magnesium oxide-coated graphene (MgO@GR) nanomaterial increases the thermal conductivity in epoxy composites [14]; 3-dimensional graphene skeletons (3DGS)

increase the tensile and compressive strengths of epoxy matrices [2]; carbon nanotubes (CNTs) wrapped with MoS_2 nano-layers (MoS_2-CNTs) provide a substantial increase in flame retardancy and thermal/ mechanical characteristics compared to the neat epoxy polymer [15]. Flame-retardant electrically conductive epoxy resin polymer nanocomposites (PNCs) were also prepared using fibril and spherical polyaniline (PANI) nanostructures as fillers [16], which increased the electrical conductivity and tensile strength of the epoxy matrix.

Although they are widely used, epoxy resins come with some limitations, in particular their high coefficient of thermal expansion (CTE), which limits their suitability for aerospace and microelectronic applications [17][18]. Zirconium tungstate (ZrW_2O_8)-based nanomaterials have been used to develop low-CTE polymer composites and they are considered for more widespread applications [19][20]. However, the fact that these nanomaterials tend to agglomerate in their respective polymer matrices limits their applications [21][22]. Recently, surface modifications using bio-based/bioinspired techniques that offer the advantage of being environmentally friendly and biocompatible have been reported [23][24]. Surface modification of ZrW_2O_8 based materials with traditional chemicals have been used to improve their mechanical and other properties. Silane coupling agents were successfully used to modify the surface of different kinds of ZrW_2O_8-based nanomaterials [25][26]. In this work, we report an easy, environmentally friendly technique to functionalize ZrW_2O_8 nano-rods employing dopamine (2-(3, 4-dihydroxyphenyl)-ethylamine) molecules. Dopamine is a synthetic equivalent of the adhesive protein found in mussels, and it exhibits the inherent ability to polymerize in basic aqueous media, forming different materials that range from polymers to ceramics [27][28]. It was successfully used for the surface modification of various nanomaterials [29][30], *e.g.*, dopamine functionalized barium titanate ($BaTiO_3$) nanoparticles exhibited enhanced dielectric properties [31]. Polyvinylidene

fluoride (PVDF)-based nanocomposites prepared using functionalized boron nitride (BNNTs) demonstrated superior thermal (CTE) and mechanical properties compared to pristine nanotube-reinforced composites [23]. In the current work, ZrW_2O_8 nano-rods synthetized using a hydrothermal method were surface-functionalized with dopamine. FTIR, TGA, Raman, XRD, SEM, and TEM techniques were used to confirm the modification of the ZrW_2O_8 nano-rods. The prime objectives of the current study were to (1) characterize the effect of dopamine on the surface characteristics of ZrW_2O_8 nano-rods and (2) investigate how functionalization affected the coefficient of thermal expansion as well as the mechanical performance of the model epoxy nanocomposites.

2. EXPERIMENTAL DETAILS

2.1 Materials

Sodium tungstate dihydrate ($Na_2WO_4 \cdot 2H_2O$) and zirconium acetate ($Zr(C_2H_3O_2)_4$) solution in dilute acetic acid (Zr 16 %) of analytical grade purity along with dopamine hydrochloride (2-(3,4-dihydroxyphenyl)ethylamine hydrochloride), 2-amino-2-hydroxymethylpropane-1,3-diol (Tris), and hydrochloric acid (36 % reagent) were procured from Sigma-Aldrich (St. Louis, MO). Bisphenol A diglycidyl ether (EPON 828) was used as a model polymer matrix; it was obtained from Hexion Specialty Chemicals, Inc. A fatty polyamide formed by tall-oil fatty acids with triethylenetetramine (Versamid 140), used as the curing agent, was acquired from Cognis/BASF (Germany).

2.2 Synthesis of ZrW_2O_8 Nano-rods

ZrW_2O_8 nano-rods were synthesized using controlled hydrothermal synthesis following the procedure reported in [32]. In brief, under hydrothermal conditions, a precursor of the nano-rods (ZrW_2O_7 $(OH)_2 \cdot 2H_2O$) was obtained by reacting 0.08 M Zr $(C_2H_3O_2)_4$ solution and 0.10 M $Na_2WO_4 \cdot 2H_2O$ in 7 M HCl at 130 °C for 12 h. After completion of the reaction, the cooled solution containing white precipitates was centrifuged for desired time intervals with deionized water to remove any residual acids, followed by drying in a vacuum oven at 75 °C for 24 h. Then white powder of ZrW_2O_7 $(OH)_2 \cdot 2H_2O$ was obtained by grinding with a mortar and pestle. Subsequently, calcination of the precursor powder at 600 °C for 30 min resulted in ZrW_2O_8 powders with nano-rod morphology.

2.3. Functionalization and Characterization of ZrW_2O_8 Nano-rods

Polydopamine (PDOPA) functionalization of the ZrW_2O_8 nano-rods (ZrW_2O_8@PDOPA) was carried out using a standard route [33]. Initially, a dopamine hydrochloride/distilled water solution was prepared under stirring at a concentration of 2.0 g l^{-1} [30]. The pH of this solution was then adjusted to 8.5 using Tris buffer, and this solution was sonicated for a minimum of thirty min until the solution turned yellow. Subsequently, the ZrW_2O_8 nano-rods were added to the solution and sonicated for an additional hour to ensure adequate dispersion of the nano-rods. The polymerization reaction was then carried out in a reflux condenser at 60 °C for another 48 h to strongly adhere the dopamine molecules to the ZrW_2O_8 nano-rods as a result of self-polymerization of dopamine. The polydopamine-functionalized nano-rods were then washed several times with distilled water and collected using a filter membrane. The functionalized nano-rods were dried in a vacuum oven at 70 °C for 24 hours. **Figure 1** shows pristine and functionalized ZrW_2O_8 nano-rods. The successful functionalization was confirmed by different

characterization techniques, including Fourier transform infrared spectroscopy (FTIR), Raman spectroscopy, thermogravimetric analysis (TGA), X-ray diffraction (XRD), field emission scanning electron microscopy (FE-SEM), and transmission electron microscopy (TEM). The FTIR spectra of pristine and functionalized nano-rod samples were recorded on a Nicolet 460 FTIR spectrometer (Madison, WI). Their Raman spectra were recorded at room temperature using a Renishaw dispersive Raman spectrometer in the range from 800 to 2000 cm^{-1}. A 480 nm solid-state laser was used as the excitation source to induce the Raman scattering effect. Small amounts of both pristine and functionalized nano-rods were uniformly deposited onto a glass slide that was physically pressed to smooth the sample prior to the measurements. The thermal stability of these samples was investigated using thermogravimetric analysis on a TA Instruments Q50 thermobalance in nitrogen atmosphere at a heating rate of 10 °C/min. X-ray diffraction (XRD) of pristine and functionalized nano-rods was carried out using a Rigaku Ultima IV powder diffractometer with Cu Kα at 40 kV/44 mA and scan steps of 0.01° from 10° to 60°. The surface morphologies of both pristine and functionalized nano-rods were characterized using field emission scanning electron microscopy (FE-SEM, FEI Quanta 200F) at 30.00 kV under high vacuum. The nano-rods were sputter-coated with a thin layer of Pt/Pd using a Cressington Sputter Coater before imaging. Detailed structure investigations of the functionalized ZrW_2O_8@PDOPA nano-rods were performed using transmission electron microscopy with a FEI Tecnai G20 Twin operating at 200 kV.

2.4 Preparation and Characterization of ZrW_2O_8/ Epoxy Nanocomposites

After drying of the pristine and functionalized nano-rods, nanocomposites were prepared by blending pristine ZrW_2O_8 and functionalized ZrW_2O_8@PDOPA nano-rods (5 wt.% loading) respectively with the model epoxy resin. The blends were sonicated employing a horn (Fisher, sonic dismembrator model 100) at 30 s intervals for 3 min with a power of 80 W; the mixtures were then cooled and the required amounts of curing agent were added. The nanocomposite mixtures were then subjected to high-speed shear mixing and degassing steps. Subsequently, the mixtures were transferred to an oven and cured at 120 °C for 16 h. The obtained epoxy-ZrW_2O_8 and epoxy/ZrW_2O_8@PDOPA nanocomposite samples were then used for further thermo-mechanical and tensile strength characterizations. The thermal expansion behavior of the pristine epoxy resin and both the ZrW_2O_8 and ZrW_2O_8@PDOPA nanocomposites was studied using a Q400 thermo-mechanical analyzer (TMA) from TA Instruments using 3 mm × 3 mm × 3 mm specimens. The tensile properties of the epoxy resin and the respective nanocomposites were determined using an Instron universal testing machine (model 4502) with a crosshead speed of 1 mm min^{-1}. The dog-bone samples were prepared and tested according to ASTM D638 using a minimum of 5 samples per batch to determine the mechanical properties.

3 RESULTS AND DISCUSSION

3.1 Functionalization of ZrW_2O_8 Nano-rods

Several organisms, especially in marine environments, are able to produce adhesives so that they strongly adhere to nearby surface[33]. Most of these organisms belong to the family of marine mussels and mussel-inspired materials have found applications because of their excellent adhesive strength, unique ability to crosslink, and moisture resistance among other properties. The adhesive and cohesive properties of the adhesive proteins in mussels are primarily attributed

to the presence of significant amounts of catecholic 3, 4-dihydroxyphenylalanine (DOPA). Unfortunately, the exact mechanism for their unique behavior is not well understood and still under investigation. Dopamine is a molecule that resembles the adhesive proteins in mussels; it contains both the catechol and amine functional groups. These groups will strongly bond/adhere to nearby surfaces under basic reaction conditions. **Figure 2 (a, b)** shows the structure of dopamine and a schematic for the polymerization of dopamine in an aqueous medium. Polydopamine adheres to many materials, ranging from ceramic to metal to polymers. When the ZrW_2O_8 nano-rods were added to the dopamine solution, dopamine adheres to the surface of the nano-rods. The change in color from white to dark brown after completion of the polymerization reaction confirms the successful functionalization of nano-rods by dopamine **(Figure 1). Figure S1** depicts the proposed polymerization mechanism of dopamine, which includes catechol oxidation to quinone, finally resulting in polydopamine [34][34]. The functionalized nano-rods were thoroughly dispersed in aqueous and organic solvents that are compatible with polydopamine molecules. The presence of –OH and NH_2 functional groups was attributed to the easy dispersion of the nano-rods in aqueous media.

3.2 Characterization of the Functionalized ZrW_2O_8 Nano-rods

We used different characterization techniques to confirm the successful dopamine functionalization of the nano-rods. **Figure 3(a, b)** shows the TEM images of pristine and functionalized nano-rods, highlighting the changes in morphology compared to the as-synthesized nano-rods. The image shows a continuous, thin, amorphous layer of polydopamine wrapped around the ZrW_2O_8 nano-rods. This layer is not seen in the pristine ZrW_2O_8 nano-rods and confirms successful functionalization. Additional SEM imaging was used to study changes in

morphology and structure of the ZrW_2O_8 nano-rods after functionalization **(Figure 4a, b)**. The figure shows there was not much difference in the structure of the pristine and functionalized nano-rods demonstrating that the 48 h polymerization stirring at high RPM does not significantly alter the dimensions of the nano-rods. The SEM images also shows that there is an increase in the nano-rods size after functionalization. Thermogravimetric analysis (TGA) measurements were carried out to determine the thermal stability of the ZrW_2O_8 nano-rods and the amount of polydopamine deposited on them **(Figure 5a, b)**. The figure shows that the pristine nano-rods were highly thermally stable up to 1000 °C. The 2.5 % weight loss seen up to 200 °C was attributed to moisture content and to hydroxy groups present in the nano-rods as a result of hydrothermal synthesis. On the other hand, polydopamine functionalized ZrW_2O_8 nano-rods exhibited slightly less thermal stability in this temperature range. This behavior was attributed to the decomposition/degradation of the polydopamine coating under high temperatures. Dopamine is thermally stable up to only 200-250 °C. In this case we can easily see the distinctive decomposition trend of polydopamine that exhibits a slow decomposition rate mass loss up to 250 °C followed by a higher rate mass loss. The amount of polydopamine coated onto the ZrW_2O_8 was determined by TGA. The thermograms showed that almost 20 wt. % of polydopamine was noncovalently coated on the ZrW_2O_8 nano-rods. **Figure 6 (a)** shows the FTIR spectra of pristine and functionalized ZrW_2O_8 nano-rods. The intensity of pristine nano-rods decreased as a result of the polydopamine functionalization, and the functionalized nano-rods exhibited several additional peaks between 1000 cm^{-1} and 1600 cm^{-1}. The presence of the peak at 1614 cm^{-1} of ZrW_2O_8@PDOPA in particular was assigned to the overlap of C═C resonance vibrations in the aromatic ring and N–H bending, while the peak at 1521 cm^{-1} was assigned to a N-H shearing vibration mode and that at 1098 cm^{-1} to the stretching mode of C-H groups

respectively, confirming the successful polymerization of dopamine. The absence of other reported bands of dopamine in the ZrW_2O_8@PDOPA spectra suggest that all dopamine molecules were successfully polymerized, which resulted in a significant decrease in intensity of pristine ZrW_2O_8 nano-rods. **Figure 6 (b)** shows the Raman spectra of pristine and functionalized ZrW_2O_8 nano-rods. Those of the pristine ZrW_2O_8 nano-rods were in agreement with the reported literature, confirming the successful synthesis of ZrW_2O_8 nano-rods [35]. The spectra also confirmed that there were no tungsten oxide impurities left in the synthesized samples. However, in comparison to the pristine nano-rods, the functionalized nano-rods exhibited a strong reduction in the overall intensity of the pristine ZrW_2O_8 nano-rods as well as absence of other smaller peaks owing to the amorphous nature of polydopamine. The Raman spectra also compliments the FTIR spectra in the sense that the intensity of characteristics peaks of polydopamine which is commonly found around 3140 cm^{-1} and 1570 cm^{-1} was reduced to significant extents. In fact it was almost impossible to distinguish them confirming the complete polymerization of dopamine into polydopamine. The ZrW_2O_8 nano-rods were also characterized by XRD **(Figure 7).** The XRD spectra of pristine nano-rods confirmed the crystalline nature of the nano-rods, while the XRD spectra of polydopamine functionalized nano-rods resembled spectra of amorphous materials with a considerable decrease in the intensities of the nano-rods, which confirmed the earlier FTIR, Raman, and TGA results.

3.3 Characterization of Polymeric Nanocomposites Using ZrW_2O_8 Nano-rods

ZrW_2O_8-based materials offer a number of advantages, including thermal stability and low coefficient of thermal expansion in advanced nanocomposites. However, the agglomeration of these ZrW_2O_8 based particles, especially in nano-dimension diminishes their properties. The

functionalization of ZrW_2O_8 nano-rods through dopamine provides a route to overcome the agglomeration issues and also provide a platform for further functionalization/ polymerization with another monomers due to presence of –OH and NH_2 functional groups. We prepared epoxy-ZrW_2O_8 and epoxy/ZrW_2O_8@PDOPA nanocomposites with 5 wt. % nano-filler loadings and studied their tensile properties and their coefficient of thermal expansion. **Figure 8 (a, b)** shows tensile strength and tensile modulus of the epoxy nanocomposites prepared with pristine and functionalized ZrW_2O_8 nano-rods. Pristine epoxy exhibited a tensile strength and modulus of 76.7 MPa and 2.78 GPa, respectively. Both tensile strength and modulus increased with the incorporation of nano-rods and the increase was more pronounced for ZrW_2O_8@PDOPA epoxy nanocomposites, which was attributed to the enhanced distribution of ZrW_2O_8@PDOPA nano-rods within the model epoxy matrix. Functionalization also allowed for good interaction between the epoxy matrix and the ZrW_2O_8@PDOPA nano-rods, which reduced the agglomerations of the nano-rods and resulted in higher tensile properties. These results are in conformity with the previous reported results as the polydopamine functionalization of ZrW_2O_8 results in the better load transfer from the model polymer matrix to ZrW_2O_8 nano-rods. **Figure 9** shows the coefficient of thermal expansion of epoxy and its respective nanocomposites with pristine and functionalized nano-rods. As expected, the incorporation of low-CTE ZrW2O8 nano-rods resulted in a decrease in CTE. It is interesting to note that for epoxy nanocomposites with functionalized nano-rods (containing 20 % PDOPA), the coefficient of thermal expansion was lower compared to that of the epoxy/ZrW_2O_8 nanocomposites. This result was explained by the fact that functionalization facilitated better interaction between the nanoparticles and the model matrix and reduced agglomeration of the nano-rods.

Conclusions

Polymer nanocomposites with suitably low coefficients of thermal expansion for certain applications were obtained. For this purpose, ZrW_2O_8 nano-rods were synthesized and functionalized in an aqueous non-solvent medium. The successful functionalization of ZrW_2O_8 nano-rods was confirmed by different characterization techniques. They were then used to create nanocomposites by incorporating both pristine and functionalized nano-rods into a model epoxy matrix. Thermal stability of the pristine and functionalized ZrW_2O_8 nano-rods was also studied. It was found that the pristine nano-rods were highly thermally stable up to 1000 °C (with only 2.5 % weight loss seen up to 200 °) while the functionalized ZrW_2O_8 nano-rods were slightly less thermal stable in the same temperature range due to the decomposition/degradation of the polydopamine coating under high temperatures. Using functionalized ZrW_2O_8 nano-rods in the nanocomposites resulted in uniform filler dispersion in the epoxy matrix, high tensile strength, and low CTE compared to pristine epoxy and epoxy/ZrW_2O_8 nanocomposites.

References

[1] H. N. Dhakal, F. Sarasini, C. Santulli, J. Tirillo, Z. Zhang, V. Arumugam, *Compos. Part - Appl. Sci. Manuf.* **2015**, *75*, 54–67.

[2] Prateek, V. K. Thakur, R. K. Gupta, *Chem. Rev.* **2016**, *116*, 4260–4317.

[3] M. C. Corobea, O. Muhulet, F. Miculescu, I. V. Antoniac, Z. Vuluga, D. Florea, D. M. Vuluga, M. Butnaru, D. Ivanov, S. I. Voicu, et al., *Polym. Adv. Technol.* **2016**, *27*, 1586–1595.

[4] C. S. Kumar, V. Arumugam, H. N. Dhakal, R. John, *Compos. Struct.* **2015**, *125*, 407–416.

[5] H. Wu, V. K. Thakur, M. R. Kessler, *J. Mater. Sci.* **2016**, *51*, 2394–2403.

[6] M. Miculescu, V. K. Thakur, F. Miculescu, S. I. Voicu, *Polym. Adv. Technol.* **2016**, *27*, 844–859.

[7] N. Burger, A. Laachachi, B. Mortazavi, M. Ferriol, M. Lutz, V. Toniazzo, D. Ruch, *Int. J. Heat Mass Transf.* **2015**, *89*, 505–513.

[8] H. Gu, S. Tadakamalla, Y. Huang, H. A. Coloradc, Z. Luo, N. Haldolaarachchige, D. P. Young, S. Wei, Z. Guo, *Acs Appl. Mater. Interfaces* **2012**, *4*, 5613–5624.

[9] R. W. Rydin, H. Y. Ma, E. T. Thostenson, *Sci. Eng. Compos. Mater.* **1998**, *7*, 269–277.

[10] H. Wu, M. Rogalski, M. R. Kessler, *Acs Appl. Mater. Interfaces* **2013**, *5*, 9478–9487.

[11] X. Zhang, O. Alloul, Q. He, J. Zhu, M. J. Verde, Y. Li, S. Wei, Z. Guo, *Polymer* **2013**, *54*, 3594–3604.

[12] L. Gao, E. T. Thostenson, Z. Zhang, T.-W. Chou, *Adv. Funct. Mater.* **2009**, *19*, 123–130.

[13] A. J. E. A. Briggs, Z. Y. Zhang, H. N. Dhakal, *J. Compos. Mater.* **2015**, *49*, 1047–1056.

[14] F. Du, W. Yang, F. Zhang, C.-Y. Tang, S. Liu, L. Yin, W.-C. Law, *Acs Appl. Mater. Interfaces* **2015**, *7*, 14397–14403.

[15] K. Zhou, J. Liu, Y. Shi, S. Jiang, D. Wang, Y. Hu, Z. Gui, *Acs Appl. Mater. Interfaces* **2015**, *7*, 6070–6081.

[16] X. Zhang, Q. He, H. Gu, H. A. Colorado, S. Wei, Z. Guo, *Acs Appl. Mater. Interfaces* **2013**, *5*, 898–910.

[17] L. C. Gallington, K. W. Chapman, C. R. Morelock, P. J. Chupas, A. P. Wilkinson, *J. Appl. Phys.* **2014**, *115*, 53512.

[18] R. F. L. Lorenzi, J. E. Zorzi, C. A. Perottoni, *J. Non-Cryst. Solids* **2014**, *403*, 102–106.

[19] Z. Peng, Y. Z. Sun, L. M. Peng, *Mater. Des.* **2014**, *54*, 989–994.

[20] L. A. Neely, V. Kochergin, E. M. See, H. D. Robinson, *J. Mater. Sci.* **2014**, *49*, 392–396.

[21] C. Lind, M. R. Coleman, L. C. Kozy, G. R. Sharma, *Phys. Status Solidi B-Basic Solid State Phys.* **2011**, *248*, 123–129.

[22] X. Chu, Z. Wu, C. Huang, R. Huang, Y. Zhou, L. Li, *Cryogenics* **2012**, *52*, 638–641.

[23] V. K. Thakur, J. Yan, M.-F. Lin, C. Zhi, D. Golberg, Y. Bando, R. Sim, P. S. Lee, *Polym. Chem.* **2012**, *3*, 962–969.

[24] V. K. Thakur, D. Vennerberg, M. R. Kessler, *Acs Appl. Mater. Interfaces* **2014**, *6*, 9349–9356.

[25] P. Badrinarayanan, M. Rogalski, H. Wu, X. Wang, W. Yu, M. R. Kessler, *Macromol. Mater. Eng.* **2013**, *298*, 136–144.

[26] G. R. Sharma, C. Lind, M. R. Coleman, *Mater. Chem. Phys.* **2012**, *137*, 448–457.

[27] H. Li, S. Chen, J. Chen, J. Chang, M. Xu, Y. Sun, C. Wu, *ACS Appl. Mater. Interfaces* **2015**, *7*, 14708–19.

[28] S. Kang, M. Baginska, S. R. White, N. R. Sottos, *Acs Appl. Mater. Interfaces* **2015**, *7*, 10952–10956.

[29] H. Wu, M. R. Kessler, *Acs Appl. Mater. Interfaces* **2015**, *7*, 5915–5926.

[30] M. Toma, G. Loget, R. M. Corn, *Acs Appl. Mater. Interfaces* **2014**, *6*, 11110–11117.

[31] M.-F. Lin, V. K. Thakur, E. J. Tan, P. S. Lee, *Rsc Adv.* **2011**, *1*, 576–578.

[32] H. Wu, P. Badrinarayanan, M. R. Kessler, *J. Am. Ceram. Soc.* **2012**, *95*, 3643–3650.

[33] H. Lee, S. M. Dellatore, W. M. Miller, P. B. Messersmith, *Science* **2007**, *318*, 426–430.

[34] F. Yu, S. Chen, Y. Chen, H. Li, L. Yang, Y. Chen, Y. Yin, *J. Mol. Struct.* **2010**, *982*, 152–161.

[35] P. Badrinarayanan, B. Mac Murray, M. R. Kessler, *J. Mater. Res.* **2009**, *24*, 2235–2242.

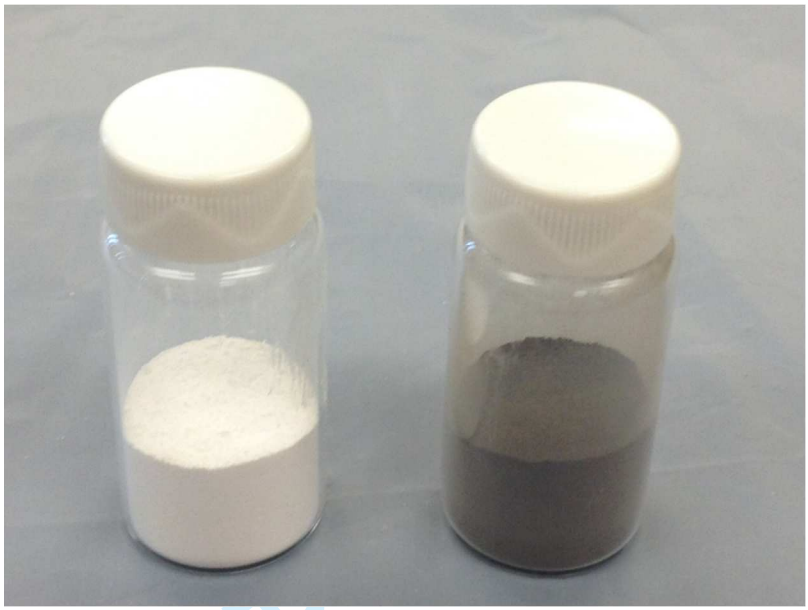

Figure 1 Photographic images of vials containing the pristine ZrW_2O_8 (white color) and the polydopamine functionalized ZrW_2O_8 (dark brown) after complete drying.

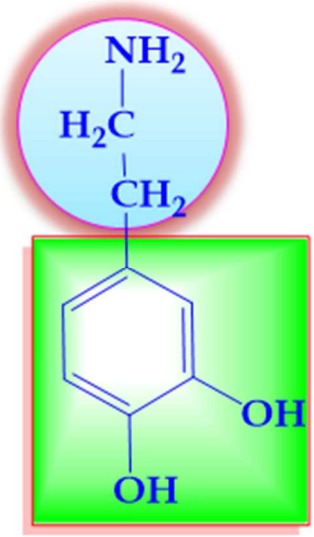

Figure 2 (a) Structure of dopamine in which green part describes catechol moiety and upper part shows alkyl amine moiety.

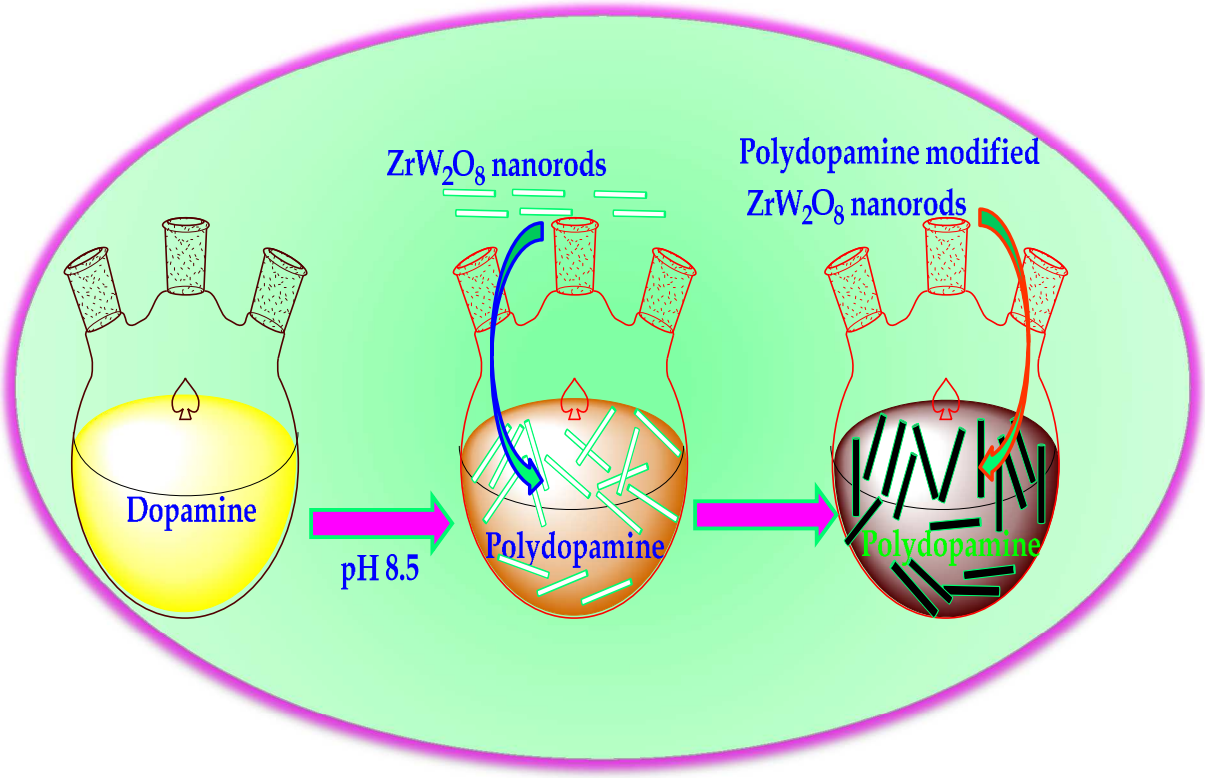

Figure 2 (b) schematic for the polymerization of dopamine onto ZrW_2O_8 nano-rods in aqueous medium.

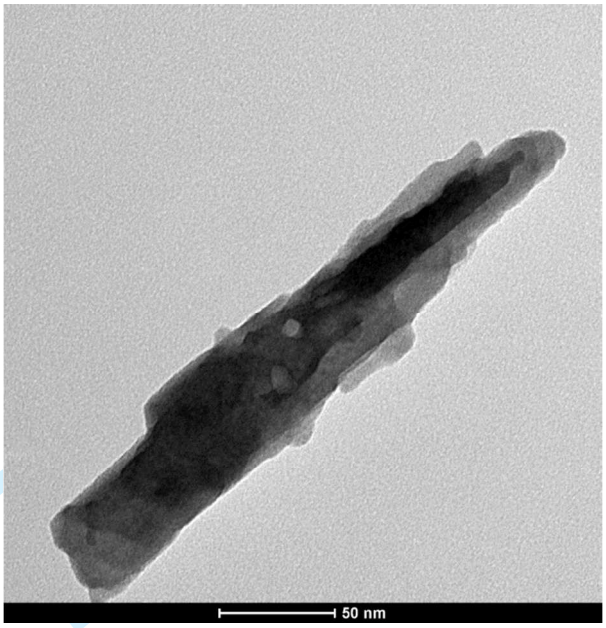

Figure 3 (a) TEM image of the pristine ZrW_2O_8 nano-rods.

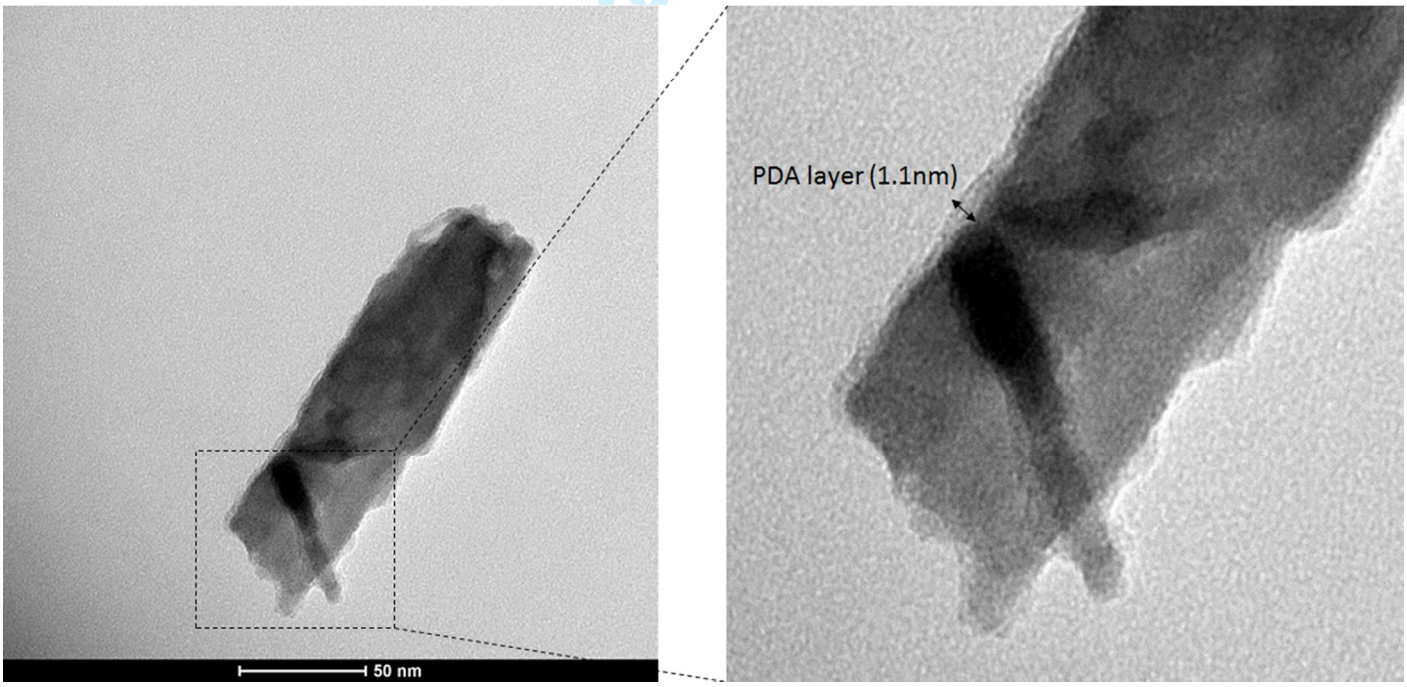

Figure 3 (b) TEM image of the ZrW_2O_8@PDOPA nano-rods.

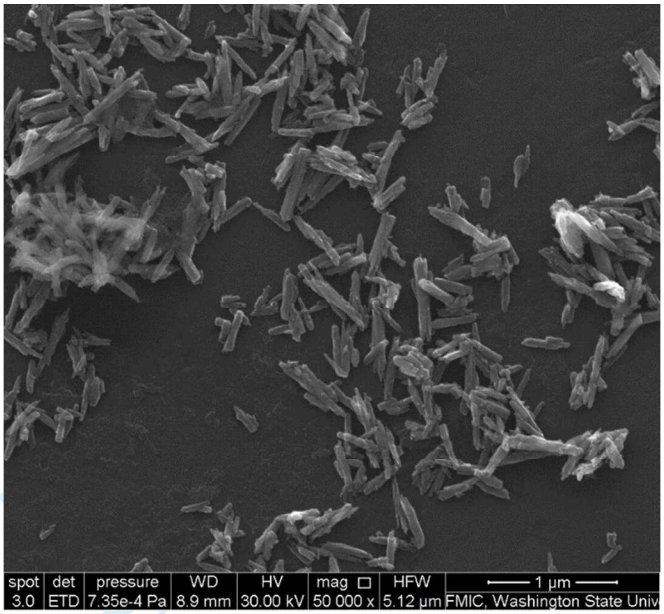

(a)

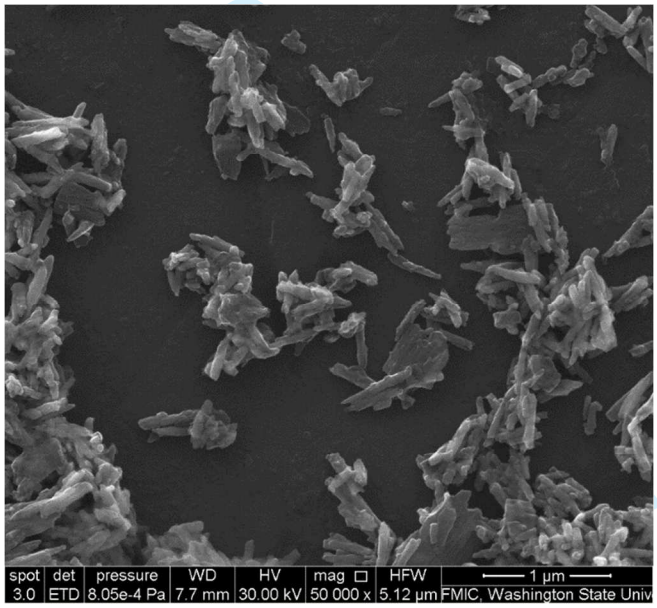

(b)

Figure 4 (a) FESEM image of pristine ZrW_2O_8 nano-rods **(b)** FESEM image of polydopamine functionalized ZrW_2O_8@PDOPA nano-rods.

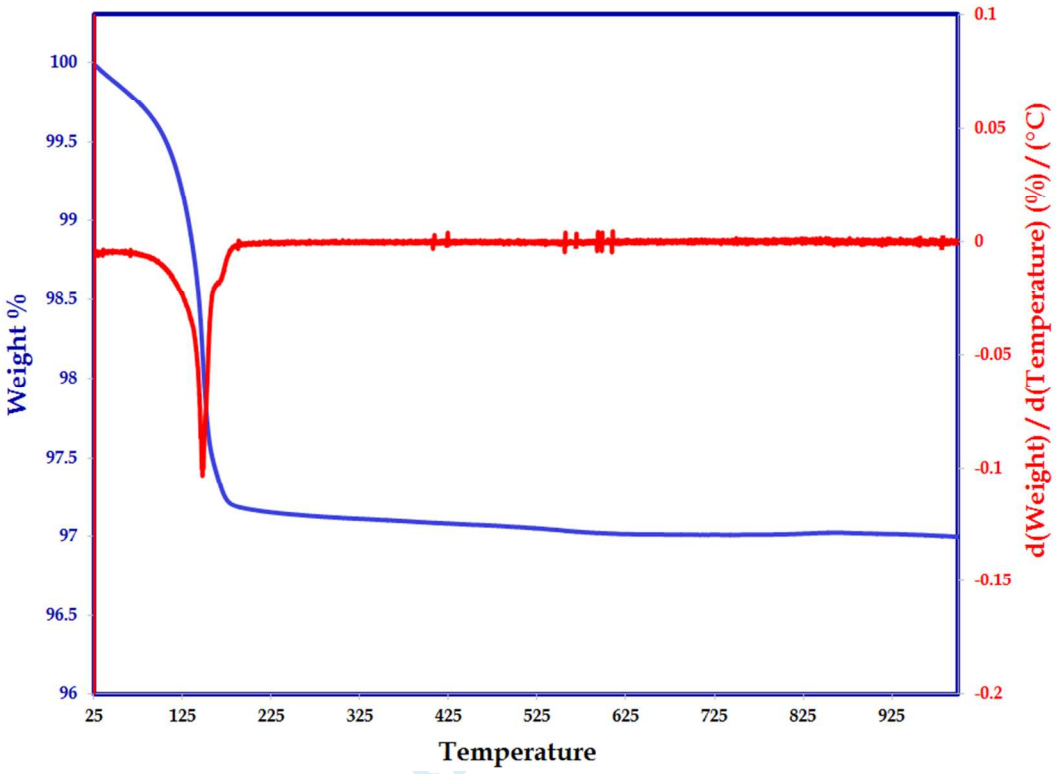

(a)

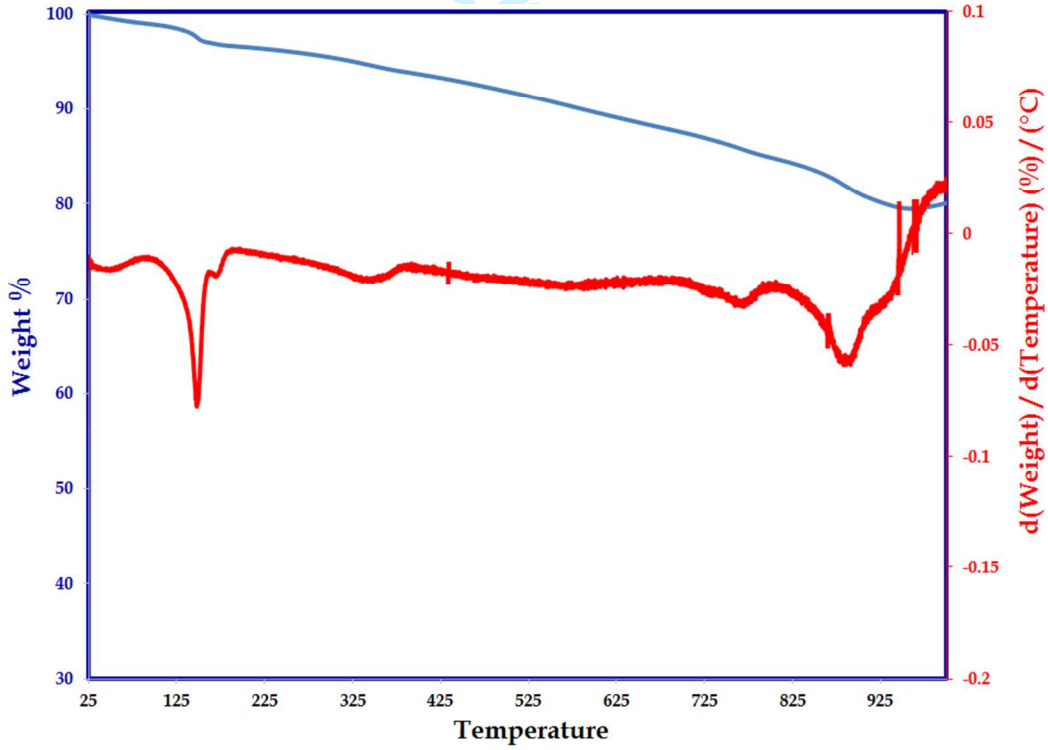

(b)

Figure 5 (a, b) TGA/ DTG curves of pristine ZrW_2O_8 and dopamine functionalized (ZrW_2O_8 @PDOPA) nano-rods.

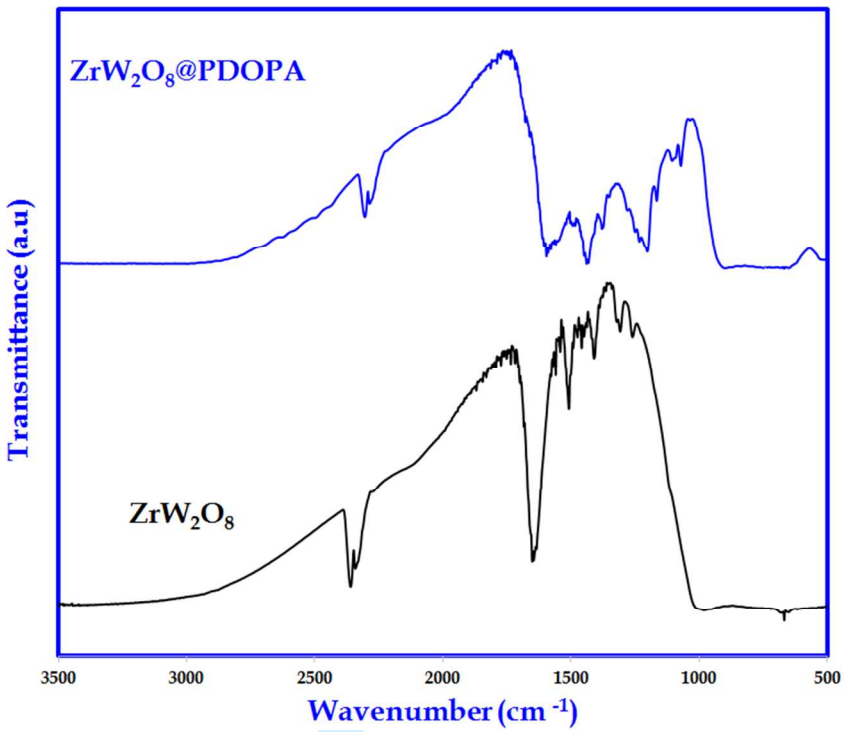

(a)

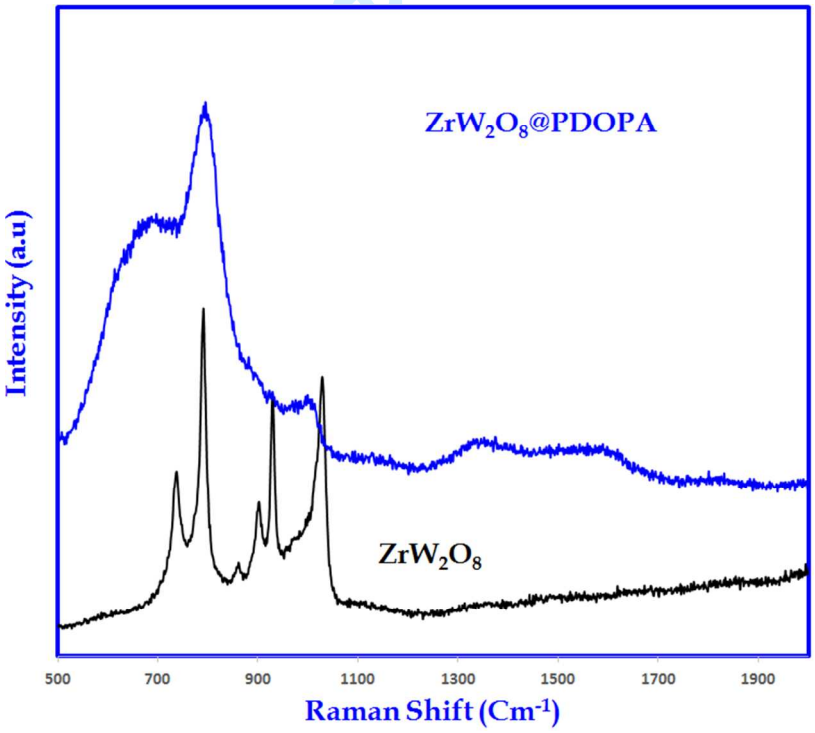

(b)

Figure 6(a, b) Comparative FTIR and Raman spectra of pristine ZrW_2O_8 and dopamine functionalized (ZrW_2O_8 @PDOPA) nano-rods.

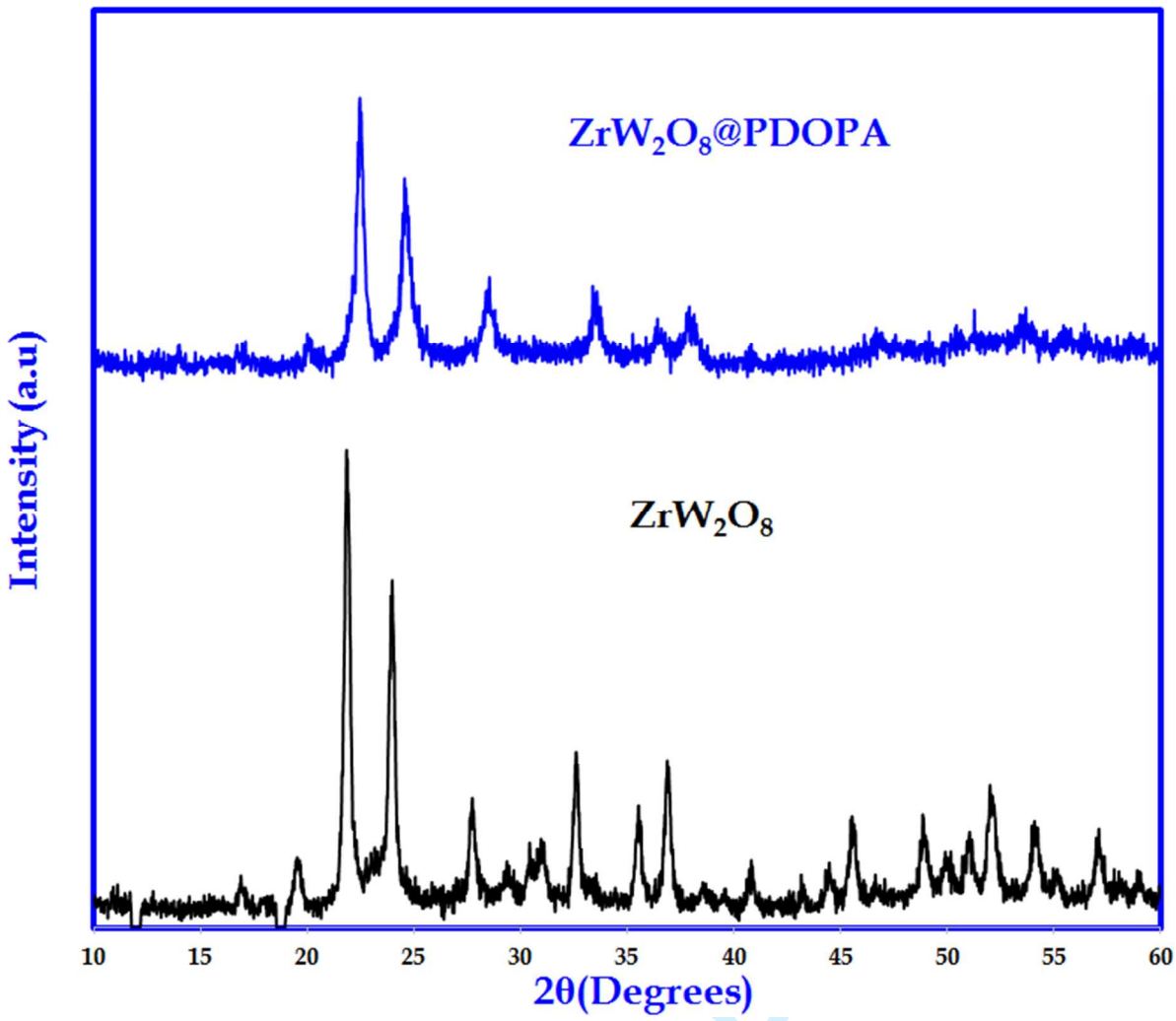

Figure 7 XRD spectrum of the product of the pristine ZrW_2O_8 and dopamine functionalized (ZrW_2O_8 @PDOPA) nano-rods.

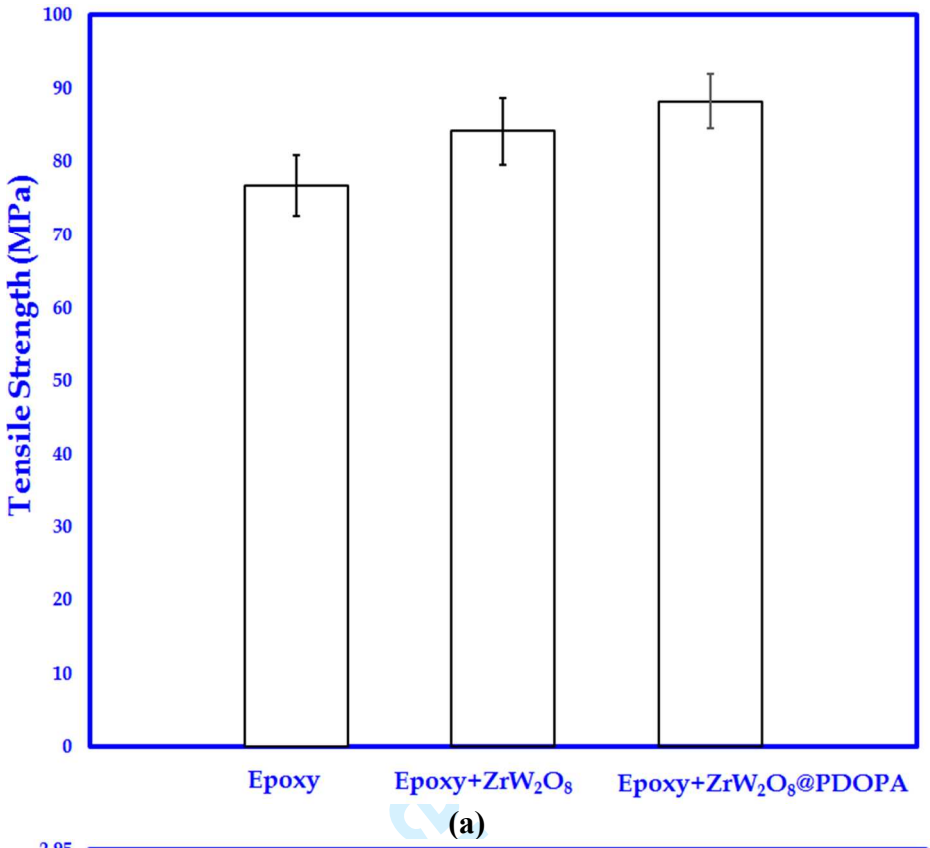

(a)

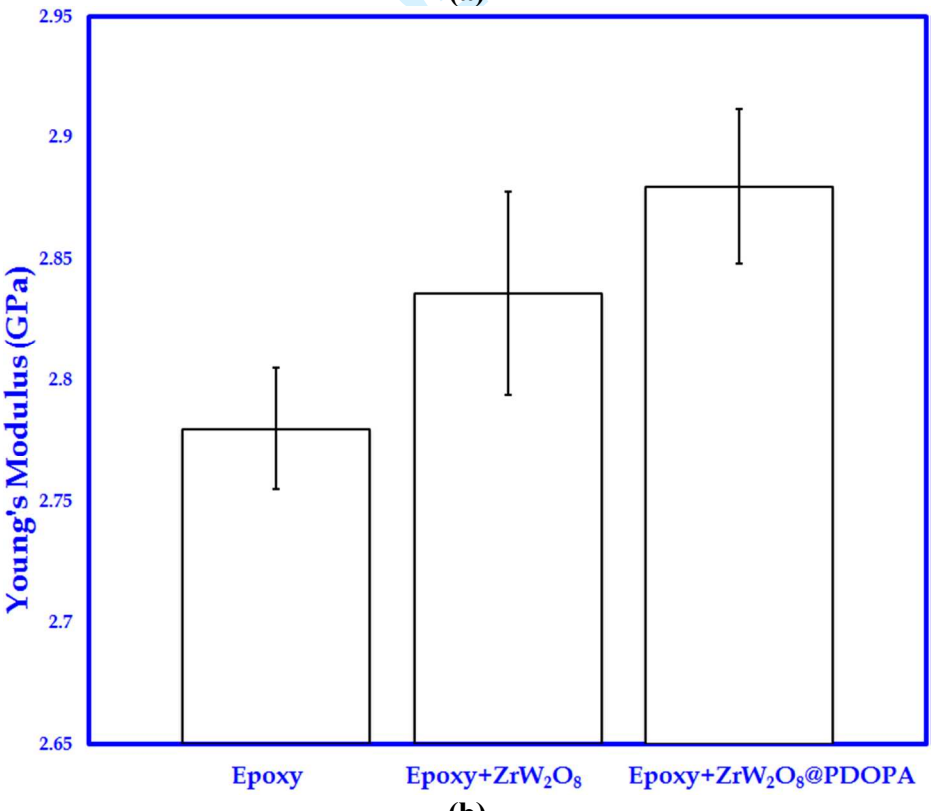

(b)

Figure 8 (a, b) Comparative tensile strength and Young's modulus results of the pristine epoxy and ZrW_2O_8/ ZrW_2O_8 @PDOPA) nanocomposites.

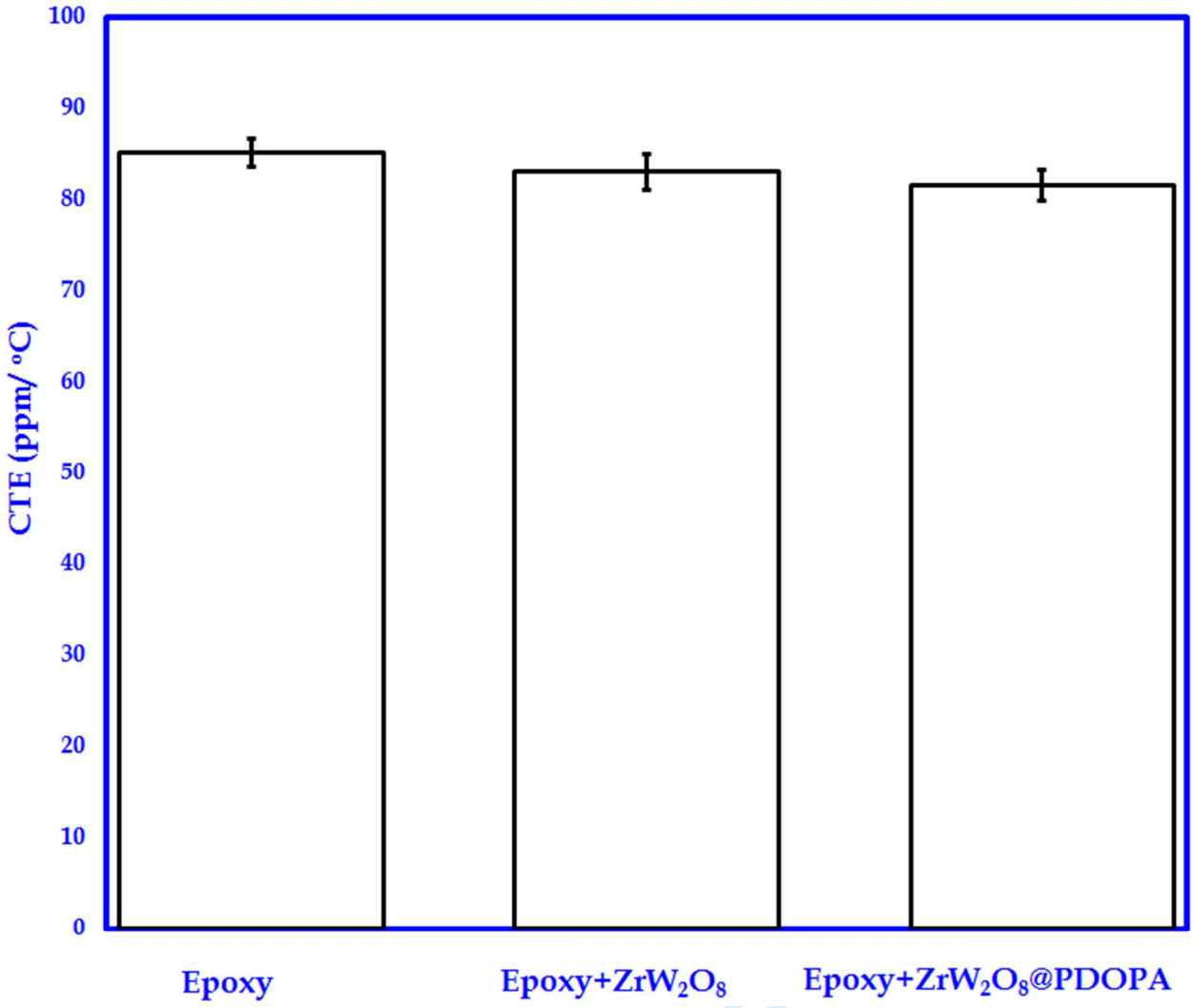

Figure 9 Coefficient of thermal expansion (CTE) results of the pristine epoxy and ZrW_2O_8/ ZrW_2O_8 @PDOPA) nanocomposites[1] [2] [3] [4].